https://doi.org/10.31436/iiumej.v26i1.3407

DEVELOPMENT OF 3D PRINTED SERPENTINE FLUIDIC CHANNEL INTEGRATED WITH HEATING ELEMENT FOR LOOP-MEDIATED ISOTHERMAL AMPLIFICATION (LAMP) PROCESS

MUHAMMAD KHAIRUL FAISAL MUHAMAD ATAN[1], ROSMINAZUIN AB RAHIM[1*], ANIS NURASHIKIN NORDIN[1], ALIZA AINI MD RALIB[1], TEDDY SURYA GUNAWAN[2], ZAINIHARYATI MOHD ZAIN[3]

[1]VLSI-MEMS Research Unit, Department of Electrical and Computer Engineering, Engineering Faculty, International Islamic University Malaysia (IIUM), Kuala Lumpur 53100, Malaysia

[2]Electrical and Computer Engineering Department, International Islamic University Malaysia (IIUM), Kuala Lumpur 53100, Federal Territory of Kuala Lumpur, Malaysia

[3]Electrochemical Material and Sensor (EMaS), Faculty of Applied Sciences, Universiti Teknologi MARA (UiTM), 40450 Shah Alam, Selangor, Malaysia

**Corresponding author: rosmi@iium.edu.my*

(Received: 17 August 2024; Accepted: 24 Sep 2024; Published online: 10 January 2025)

ABSTRACT: DNA-based point-of-care (POC) diagnostics require rapid, accurate, and portable platforms for detection of infectious diseases. This can be achieved by incorporating a loop-mediated isothermal amplification (LAMP) process for DNA amplification into the system. LAMP offers a promising in-situ solution, but maintaining consistent reaction conditions, such as a constant temperature, specifically at 65°C for 35 minutes to complete the LAMP process, remains a critical challenge. Therefore, this work presents the development of a 3D-printed serpentine fluidic channel integrated with a heating element for DNA amplification through the LAMP process. To assess their heating capabilities, heating testing was initially performed on several commercially available heating elements (Heater Cartridge, PTC 140, and PTC 230). PTC 230 heating element was chosen for its rapid heating performance (reaching 65°C in 54.78 seconds). Later, three serpentine fluidic channels of different diameters (1.6 mm, 1.7 mm, and 1.8 mm) were fabricated using a Masked Stereolithography Apparatus (MSLA) 3D printer. The developed portable LAMP device consisting of a fabricated serpentine fluidic channel on a PTC 230 heating element allows the sample to be heated at 65°C for 35 minutes. Sample flow inside each serpentine fluidic channel was measured and compared with the expected flow time of 35 minutes. It was observed that the fluidic channel with a 1.6 mm diameter shows the closest value of 34.33 minutes (percentage deviation of 1.91%) as compared to the other two channels. The optimized fluidic channel design (channel diameter of 1.6 mm) coupled with the rapid heating performance of the PTC 230 element (reaching 65°C in 54.78 seconds) for a portable LAMP device represents a significant step towards developing rapid, accurate, and portable POC diagnostic tools.

***ABSTRAK*:** Diagnostik point-of-care (POC) berasaskan DNA memerlukan platform yang pantas, tepat, dan mudah alih untuk mengesan penyakit berjangkit. Ini boleh dicapai dengan menggabungkan proses penguatan isoterma bersandar gelung (LAMP) ke dalam sistem untuk penguatan DNA. LAMP menawarkan penyelesaian in-situ yang menjanjikan, tetapi mengekalkan keadaan reaksi yang konsisten, seperti suhu tetap pada 65°C selama 35 minit untuk menyelesaikan proses LAMP, kekal sebagai cabaran kritikal. Oleh itu, kajian ini membentangkan pembangunan saluran bendalir berlingkar 3D yang dicetak dengan integrasi

elemen pemanas untuk penguatan DNA melalui proses LAMP. Untuk menilai keupayaan pemanasannya, ujian pemanasan dijalankan pada beberapa elemen pemanas komersial yang tersedia (Heater Cartridge, PTC 140, dan PTC 230). Elemen pemanas PTC 230 dipilih kerana prestasi pemanasannya yang pantas (mencapai 65°C dalam 54.78 saat). Selepas itu, tiga saluran bendalir berlingkar dengan diameter berbeza (1.6 mm, 1.7 mm, dan 1.8 mm) telah dihasilkan menggunakan pencetak 3D Masked Stereolithography Apparatus (MSLA). Peranti LAMP mudah alih yang dibangunkan, terdiri daripada saluran bendalir berlingkar yang dihasilkan di atas elemen pemanas PTC 230, membolehkan sampel dipanaskan pada suhu 65°C selama 35 minit. Aliran sampel di dalam setiap saluran bendalir berlingkar diukur dan dibandingkan dengan masa aliran yang dijangkakan selama 35 minit. Didapati bahawa saluran bendalir dengan diameter 1.6 mm menunjukkan nilai yang paling hampir iaitu 34.33 minit (peratusan sisihan 1.91%) berbanding dua saluran lain. Reka bentuk saluran bendalir yang dioptimumkan (diameter saluran 1.6 mm) digabungkan dengan prestasi pemanasan pantas elemen PTC 230 (mencapai 65°C dalam 54.78 saat) untuk peranti LAMP mudah alih mewakili langkah signifikan ke arah pembangunan alat diagnostik POC yang pantas, tepat, dan mudah alih.

KEYWORDS: *3D printing, fluidic channel, heating element, loop-mediated isothermal amplification (LAMP)*

1. INTRODUCTION

Rapid and accurate DNA-based point-of-care diagnostics are essential for effectively managing infectious diseases. Isothermal nucleic acid amplification techniques, such as loop-mediated isothermal amplification (LAMP), are frequently used to detect various molecules, including RNA, DNA, and proteins in infectious diseases [1]. Unlike the gold-standard polymerase chain reaction (PCR), LAMP provides faster and simpler alternatives, making them well-suited for use in resource-limited settings [2, 3]. Although LAMP holds promise for portable diagnostics, challenges persist in fulfilling its requirements, such as managing small liquid volumes and maintaining a consistent heating temperature. For example, to detect the COVID-19 virus, the LAMP process must maintain a constant temperature of 65°C for 35 minutes to amplify the DNA [4]. The virus can be detected using a portable potentiostat by amplifying the targeted genetic material of DNA in a fluidic sample [4].

Fluidics are crucial in analytical chemistry because they offer advantages in reagent consumption, waste reduction, process integration, and cost efficiency. Previous researchers have developed a microfluidic-based nucleic acid detection platform that uses circular reaction chambers for the LAMP process [5–8]. Lin et al. developed a chip that can perform multiplex testing with three microchannels and 18 circular chambers and is powered by capillary force, eliminating the need for valves or pumps [5]. In another work, Ma et al. presented a self-driven microfluidic chip using digital LAMP for rapid and automated DNA quantification, achieving a 30-minute amplification with an 11-copy limit of detection [6]. Yu et al. introduce a self-partitioning SlipChip (sp-SlipChip) microfluidic device for a robust droplet generation in digital LAMP, enabling point-of-care quantitative analysis of human papillomavirus (HPV) DNA [7]. Another work reported by Sun et al. demonstrated a smartphone-integrated point-of-care system for rapid and specific detection of live viruses in nasal swab samples using LAMP on a microfluidic chip, achieving accurate diagnoses with a limit of detection comparable to traditional PCR tests in about 30 minutes [8]. The mentioned research works have demonstrated the integration of microfluidic devices for the LAMP process. However, most developed microfluidic devices utilize complex fabrication methods, limited design flexibility, and material constraints [9].

https://doi.org/10.31436/iiumej.v26i1.3407

There is growing interest in exploring alternative fabrication techniques to address these limitations. 3D printing is identified as a promising alternative to developing microfluidic devices due to its simpler fabrication method, cost-effectiveness, and customizable fluidic channels [10]. In addition, testing-based optimization is feasible with 3D printing because designs can be easily modified and reprinted [11]. Furthermore, 3D printed devices can be produced without a cleanroom environment, and most importantly, 3D printing is inexpensive because the only consumables required is the filament [12]. Lastly, 3D printing fully utilizes all three dimensions in device architecture, enabling the development of innovative and unique capabilities [13]. 3D printing is a method of fabricating layer by layer consisting of three main stages. The first stage involves designing the structure using computer-aided design (CAD) software and exporting the design in stereolithography (STL) format. The second stage involves using slicer software to convert the STL file into G-code, which is tailored to the specific settings of the 3D printer. The third stage is the actual 3D printing process, where the printer uses the G-code to construct the object layer by layer according to its resolution. Various 3D printing methods are available, which include fused deposition modeling (FDM), stereolithography (SLA), digital light processing (DLP), and selective laser sintering (SLS).

Therefore, this work presents the development of a 3D-printed serpentine fluidic channel integrated with a heating element for DNA amplification through the LAMP process. Integrating a 3D-printed fluidic channel offers advantages in terms of design flexibility, rapid prototyping, and potential cost reduction compared to traditional microfabrication techniques [14]. The combination of a heating element and a fluidic channel system in a portable LAMP device allows all the necessary processes (DNA amplification, detection, and quantification) to be done in a single POC device. This paper is organized as follows: The design of the fluidic device is addressed in Section 2, where the design specifications required for LAMP and the calculation of dimension and flow rate are described. Section 3 discusses the experimental work, the fabrication process, and the functional testing of the fluidic device. Section 4 discusses the result of this work. Finally, the summary of this study is presented in Section 5.

2. DESIGN CONCEPT OF PORTABLE LAMP DEVICE

The design of the portable LAMP device, as illustrated in Figure 1, is meticulously engineered to ensure efficiency, accuracy, and portability. Figure 1(a) presents an exploded view of the connector lid, which houses several crucial components: the fluidic device, the PTC heating element, and the sensor holder. The PTC heating element maintains the temperature required for the LAMP process, while the fluidic device ensures proper sample flow. The sensor holder securely positions the sensor, facilitating accurate data acquisition. This modular arrangement enables easy assembly and maintenance, improving overall usability. Figure 1(b) depicts the fully assembled portable LAMP device, which integrates the connector lid assembly and the sensor holder assembly into a compact unit. Four strategically placed magnets on the connector lid reinforce the connection between these two assemblies. These magnets ensure secure attachment and enable seamless connectivity between the wire and the connector. The wire and connector link the sensor's electrodes to the potentiostat board, essential for processing the electrochemical signals generated during the LAMP process. This streamlined connection enhances the device's performance and minimizes potential signal loss. Figure 1(c) provides an exploded view of the sensor holder, which consists of the sensor, the sensor holder itself, and the PDMS sample well. The PDMS sample well is critical, as it channels the fluidic sample toward the sensor’s electrodes while preventing leakage. This precise flow control ensures that the sample remains intact and accurately reaches the sensor. Furthermore, the sensor holder assembly firmly secures the sensor and the sample well, preventing displacement

https://doi.org/10.31436/iiumej.v26i1.3407

during the LAMP process. This cohesive design highlights the device's reliability, ensuring precise operation, efficient heat distribution, and secure sample handling, making it a significant advancement in portable diagnostic tools.

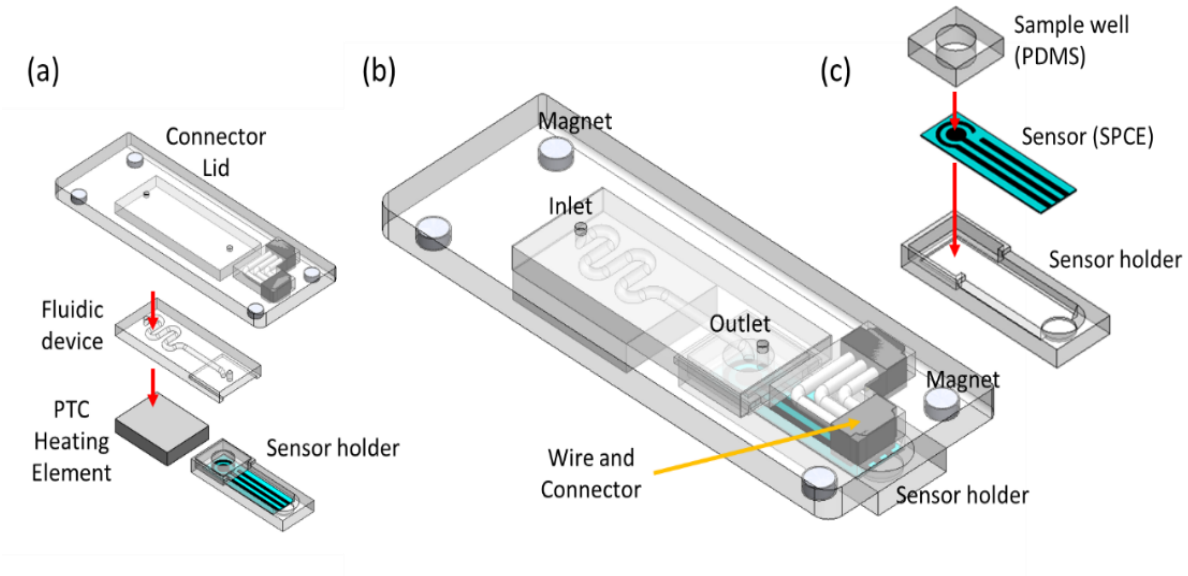

Figure 1. Design of portable LAMP device. (a) An expanded view of the assembly within the connector lid: PTC heating element, fluidic device, and connector lid. (b) Complete design of portable LAMP device consisting of the assembly within the connector lid and the assembly within the sensor holder (c) Exploded view of the assembly within the sensor holder: sensor holder, sensor, and sample well.

2.1. LAMP Specification

To complete the LAMP reaction for DNA amplification, a constant temperature of 65°C must be maintained for 35 minutes to optimize the amplification process [4]. A fluidic device was designed to transport fluidic samples to the screen-printed carbon electrode (SPCE) sensor while maintaining the temperature required for the LAMP reaction to complete. Optimizing the fluidic channel specifications is crucial for optimal fluid flow. The selection of the heating element is vital for accurate temperature regulation. Although the LAMP process typically utilizes sample volumes of 10 to 20 µL [15–17], the circular detection area of the SPCE requires a larger sample volume of 50 to 200 µL for sufficient coverage and measurement [18–20]. The volume range of 50 to 200 µL will be used for our design to ensure adequate signal detection and complete LAMP amplification results.

The fluidic channels, chambers, and structures are designed based on the fundamental principles of fluid dynamics and heat transfer. The serpentine configuration of the channel on top of the heater creates an extended fluid-path length, maximizing the thermal interaction between the sample and the heater surface. This design promotes efficient and uniform sample heating throughout the 35-minute heating process. The dimensions of the channels are carefully selected to control the sample volume to ensure accurate fluid handling. The outlet of the serpentine channel, strategically positioned above the sensor, enables rapid and direct delivery of the heated sample to the sensor area, facilitating real-time analysis and detection.

https://doi.org/10.31436/iiumej.v26i1.3407

2.2. Design of Fluidic Channels

The fluidic channels of various diameters were designed to test the MSLA 3D printer's capabilities in fabricating small-sized structures. A test design consisting of a linear arrangement of seven channels, each with a diameter ranging from 1.1 to 1.7 mm with 5 mm spacing, is shown in Figure 2. The channels, measuring 55 mm in length and 3 mm in thickness, were designed to facilitate sufficient heat transfer during the LAMP process while achieving printable dimensions of fluidic channels.

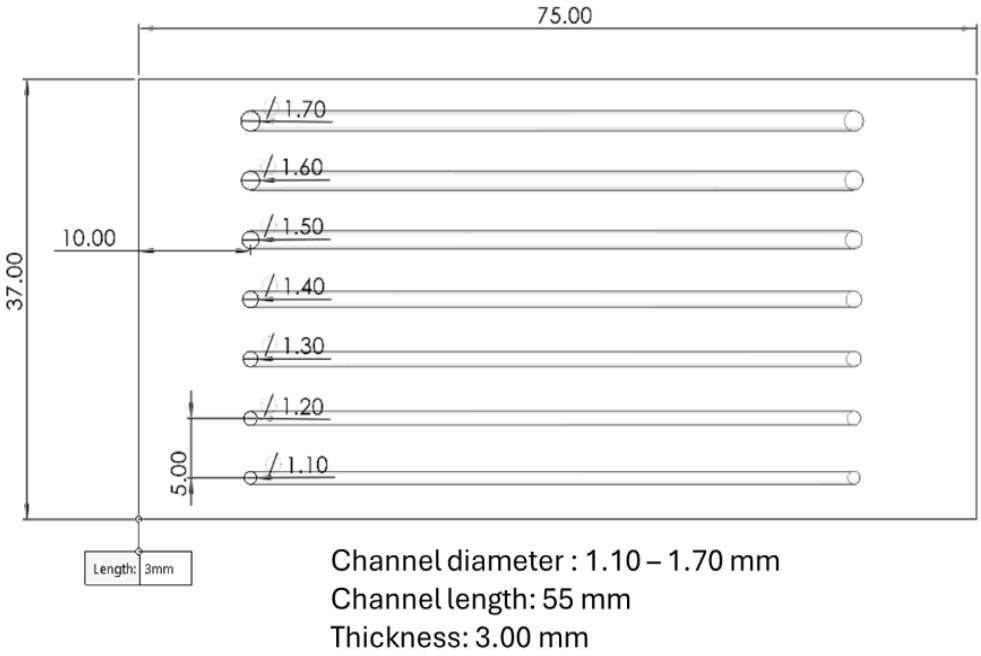

Figure 2. The test design consists of 7 channels with varying diameters (1.10 - 1.70 mm) and 55 mm channel length.

2.3. Fluidic Volume Calculation

The following equation was used to determine the sample volume flowing in the channel,

$$V = \frac{\pi D^2 l}{4} \quad (1)$$

where D is the diameter and l is the length of the channel (both in mm). This equation assumes that the fluidic channel has a circular cross-sectional area. The volume is calculated as the product of the cross-sectional area ($\frac{\pi D^2}{4}$) and the channel length (l). The calculated volumes of the serpentine channels are 93.61 ml to 118.48 ml, as shown in Table 1 in Section 3.2, together with the measured values.

3. EXPERIMENTAL WORKS

This section discusses the experimental works on fluidic channel fabrication, volume measurements, and heat distribution measurements. The fabricated fluidic devices will be tested with red-colored fluid (representing sample fluid) to observe fluid flow time within the serpentine channel. Heating elements will be tested with an Arduino microcontroller to determine the time required to reach the desired temperature.

https://doi.org/10.31436/iiumej.v26i1.3407

3.1. Fabrication of Fluidic Channels

The fluidic channel was fabricated using mask stereolithography (MSLA) with a Phrozen Sonic Mini 8K 3D printer. This high-resolution 3D printing technique uses UV light to cure a liquid photopolymer resin, resulting in exceptional detail and precision, making it ideal for crafting intricate fluidic devices. The printer's 8K resolution LCD panel contributes to improved accuracy and speed at an affordable cost. PMMA-like resin, selected for its fluid visualization capabilities, smooth surface properties, and biocompatibility, served as the primary material for the fluidic channel.

To achieve optimal fluidic channel formation, the exposure time for the MSLA process was determined through experimentation. The fluidic design file was uploaded to the printer, followed by resin being loaded into the printer's tank. The printer then initiated the curing process, solidifying the resin layer by layer according to the uploaded design. Upon completion, the printed part was immersed in isopropyl alcohol (IPA) for 4 minutes to remove excess resin. Afterward, it was exposed to UV light for 5 minutes to improve its mechanical properties and stability.

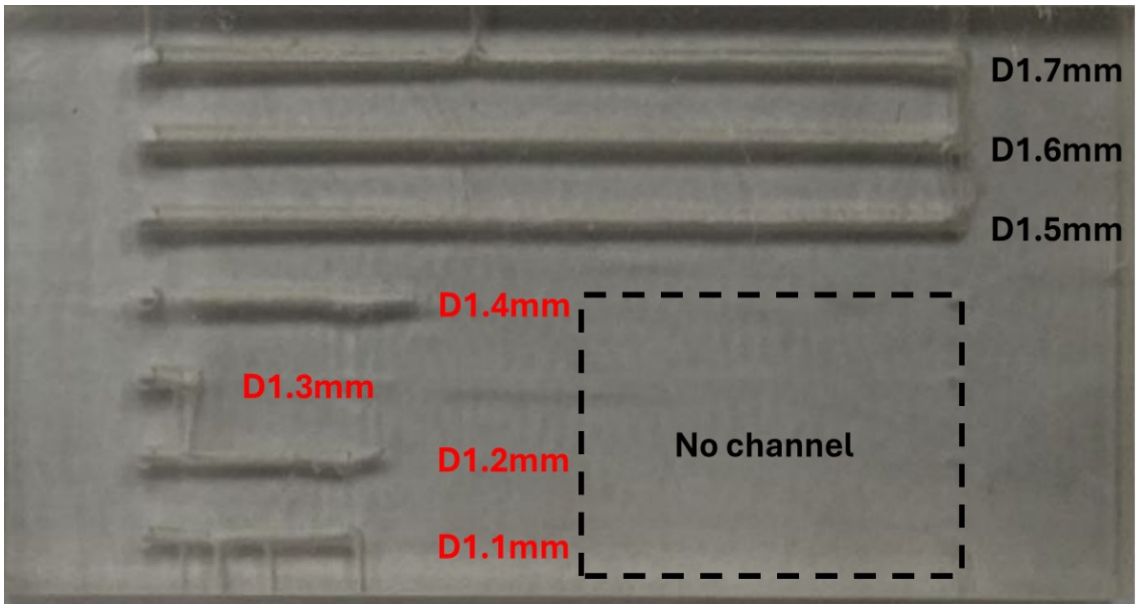

Figure 3. The fabricated fluidic channels of the test designs (channel length 55 mm) with a 5 mm gap between the channels for channel diameters ranging from 1.1 mm to 1.7 mm.

Figure 3 shows the fabricated fluidic channels of 55 mm length for channel diameters ranging from 1.1 mm to 1.7 mm. It was observed that the fluidic channels with diameters smaller than 1.5 mm were not fully formed, which indicates that the minimum printable channel diameter for this test design is 1.5 mm. Therefore, for subsequent fabrication, the smallest channel diameter was set at 1.6 mm to ensure full formation of channels can be achieved. Considering the printer's printing capability, the design of the fluidic channel is set as 50 mm x 20 mm x 4 mm (L × W × H), as shown in Figure 4(a). The heater area is where the heating element was placed (exactly below the fluidic device) to ensure uniform heating. An isometric view of the fluidic channel in Figure 4(b) shows the three-dimensional structure of the serpentine-shaped channel. Three-channel diameters of 1.6 mm, 1.7 mm, and 1.8 mm were chosen for performance comparison. To achieve a complete LAMP process, the channels were

https://doi.org/10.31436/iiumej.v26i1.3407

designed in a serpentine shape above the heater area to allow the sample volume to flow and stay on top of the heater while being heated at 65° for 35 minutes. As shown in Figure 4(c), the fluidic channel with a channel diameter of 1.7 mm was successfully fabricated using an MSLA printer. The length of the serpentine channel inside the heater area (from A to B) is 46.82 mm. The details of the fabricated fluidic channels' dimensions will be discussed in Section 4.1.

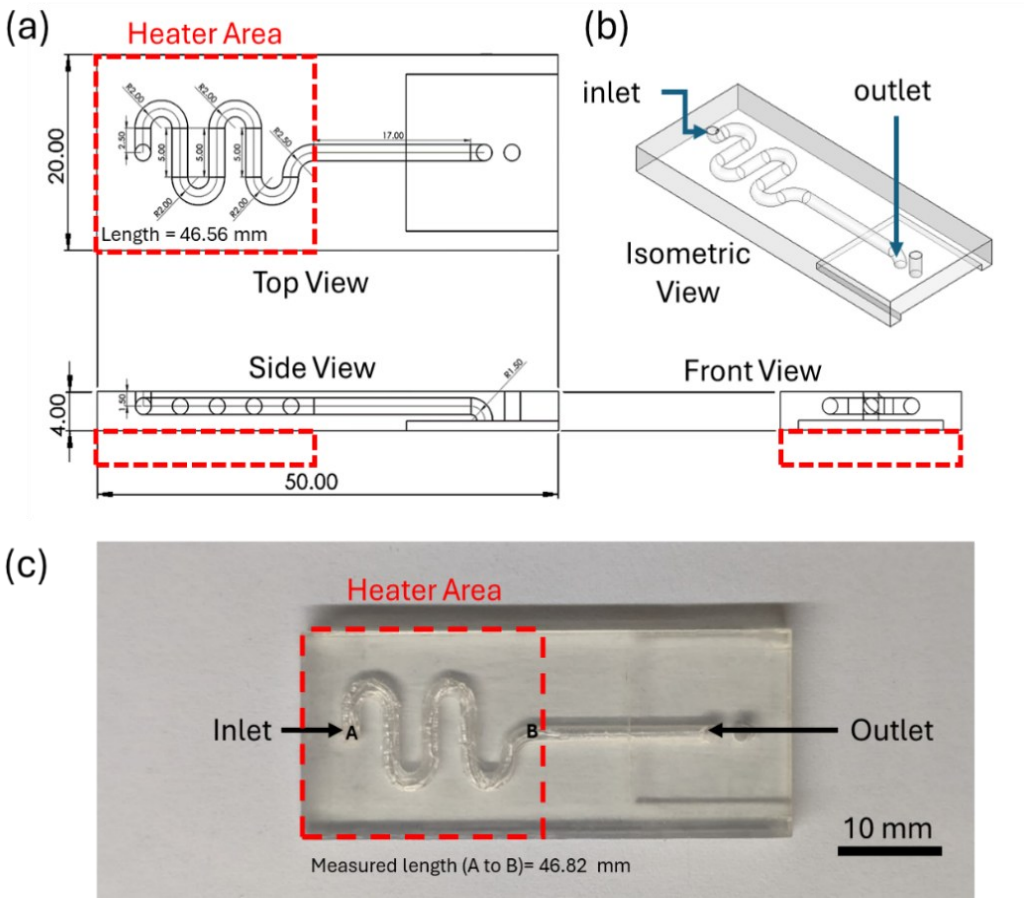

Figure 4(a) The fluidic device design uses SolidWorks 2022 (dimensions are millimeters). (b) Isometric view showing the three-dimensional structure of the serpentine-shaped channel. (c) Fabricated fluidic channel using an MSLA 3D printer with a measured channel length of 46.82 mm.

3.2. Experimental Setup for Fluidic Device

The experimental setup shown in Figure 5 was used to test the fabricated fluidic device's functionality and measure the channel's flow time. The setup comprises a syringe pump (NE-300, New Era Pump Systems, Inc), a small tube, the fabricated fluidic device, red-colored fluid to represent the fluidic samples, a heating element, and a digital microscope (Dino-Lite). The syringe pump was connected to the inlet of the fabricated channels via a small tube. The syringe pump was utilized to control the flow rate of the red-colored fluid into the fluidic channels. The Dino-Lite Digital Microscope was employed to track the flow time of the fluidic sample reaching the outlet. As depicted in Figure 5, the inset shows the flow of red-colored fluid inside the fabricated serpentine fluidic channel. The time for the fluid to flow from A to B was recorded on a computer for analysis.

https://doi.org/10.31436/iiumej.v26i1.3407

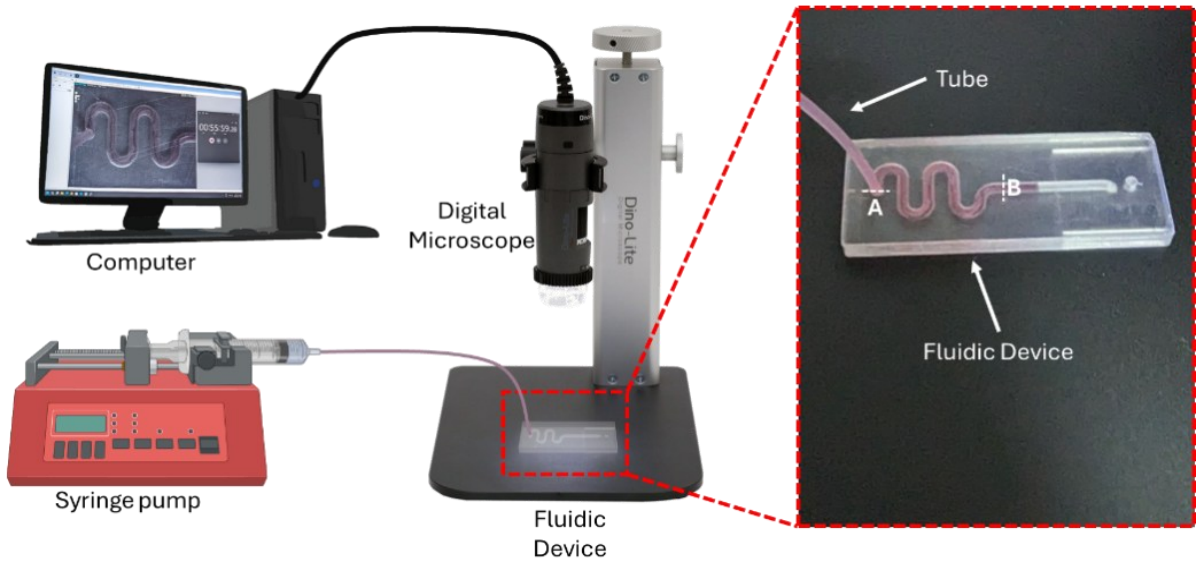

Figure 5. An experimental setup for fluid flow analysis consists of a fluidic device, a syringe pump, and a digital microscope connected to a computer.

Fluidic channels of varying diameters were configured with different flow rates to guarantee a 35-minute fluidic flow from point A to point B for all channels. For channel diameters of 1.6 mm, 1.7 mm, and 1.8 mm, the initial flow rates were established at 2.67 µl/min, 3.02 µl/min, and 3.39 µl/min, correspondingly. The video recording of the fluidic flow commenced immediately after the syringe pump was initiated to pump the fluid. The time interval between the fluid reaching point A and point B determines the flow time.

Table 1 shows the calculated volumes for each channel diameter are 1.6 mm, 1.7 mm, and 1.8 mm. The volume of the device's fluidic sample is 93.61 mm³ for the 1.6 mm diameter channel, 105.68 mm³ for the 1.7 mm diameter channel, and 118.48 mm³ for the 1.8 mm diameter channel. As previously mentioned, these values align with the standard range of 50 to 200 mm³ for fluidic sample volumes utilized with SPCE sensors [16–18].

Table 1. Calculated volume within the serpentine fluidic channel for each channel diameter

Channel diameter [mm]	Channel Length [mm]	Calculated Volume [mm^3] (Eq. 1)
1.6	46.56	93.61
1.7	46.56	105.68
1.8	46.56	118.48

3.3. Heat Distribution Measurements

Measuring the heating elements' temperatures is crucial to achieve a constant temperature of 65°C. Figure 6(a) shows the experimental setup that evaluated the heaters' capabilities by testing the heating elements using a 5V power supply derived from a USB C module. An Arduino microcontroller is connected to a MAX6675 thermocouple to measure the temperature of the heating elements powered by a 5 V USB-C module. The chosen heating elements are a heater cartridge (HC) and two positive temperature coefficient (PTC) heaters, as shown in Figure 6(b). The comparison was done by observing the time taken for each heating element

https://doi.org/10.31436/iiumej.v26i1.3407

to reach 65°C. PTC 230 was chosen as it took the least amount of time of 54.78 s compared to the other heating elements. The specifications of each heating element are listed in Table 2.

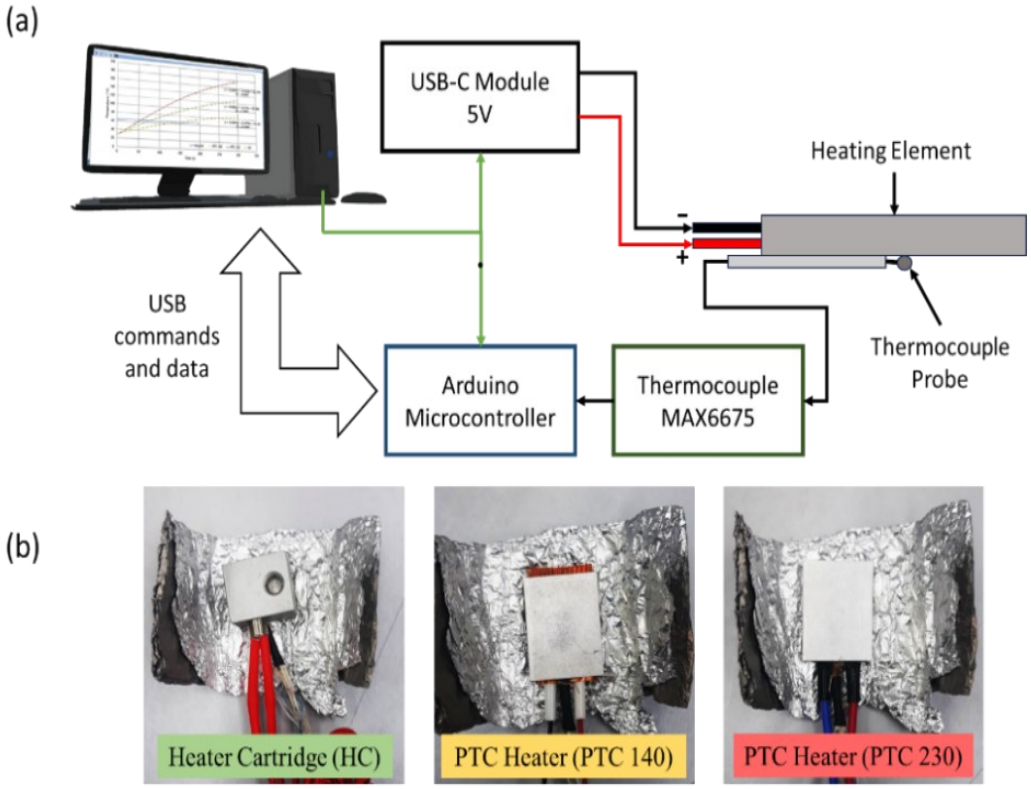

Figure 6(a) Block diagram of the experimental setup used to validate the functionality of the heating elements. (b) The different heating elements tested in the experiment: Heater Cartridge (HC), PTC Heater (PTC 140), and PTC Heater (PTC 230).

Table 2. Specification of heating elements

Heating Element	Max Temperature [°C]	Voltage [V]	Power [W]	Heater size [mm]
Heater Cartridge	300	12	40	20 x 11.5 x 16
PTC heater 140	140	12	12	20 x 20 x 5
PTC heater 230	230	12	12	20 x 20 x 5

The comparison was done by observing each heating element's time to reach 65°C. PTC 230 was selected for its shortest time of 54.78 seconds compared to the other heating elements. Details of the results will be discussed in Section 4.2. After the suitable heating element based on the rapid heating profile, the uniformity of heat distribution was analyzed using an infrared thermal imaging analyzing camera, Super Cam X (QianLi, China). The thermal camera was positioned directly on top of the heating element, and the heat distribution was observed from room temperature to a maximum temperature of 65°C. The thermal camera was connected to a computer, and the images were captured and analyzed using QianLi IR software. The heat distribution results are discussed in Section 4.2.

https://doi.org/10.31436/iiumej.v26i1.3407

4. RESULTS AND DISCUSSION

This section discusses the results of flow time measurement and heat distribution testing for selected heating elements.

4.1. Measurement Results for the Flow Time of the Fluidic Sample

Figure 7(a) shows the inset of the fluidic sample flowing inside the channel (from A to B) in 34 minutes 30 seconds ((Time at B) minus (Time at A)). Figure 7(b) shows the red-colored fluid flowing from the fluidic device into the PDMS sample well in the sensor holder. No leakage was observed during the measurement of the flow time of the fluidic sample.

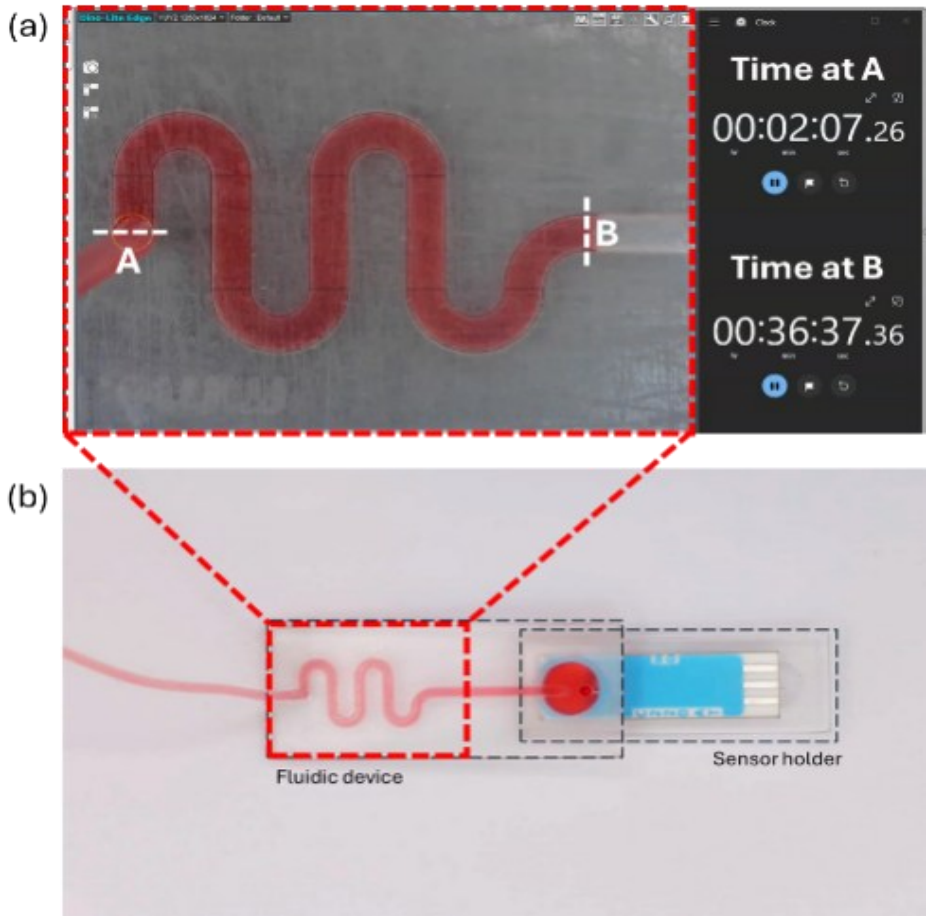

Figure 7(a) The inset of red-colored fluid flows within the channel without leakage and takes 35 minutes to complete its flow. (b) The flow of red-colored fluid in the fluidic channel into the PDMS sample well in the sensor holder.

Three fluidic channels of varying channel diameters (1.6 mm, 1.7 mm, and 1.8 mm) with the same channel length of 46.56 mm (from A to B) were 3D printed using an MSLA printer, as shown in Figure 8. The length and diameter of 3D-printed fluidic channels were measured by DinoCapture software.

https://doi.org/10.31436/iiumej.v26i1.3407

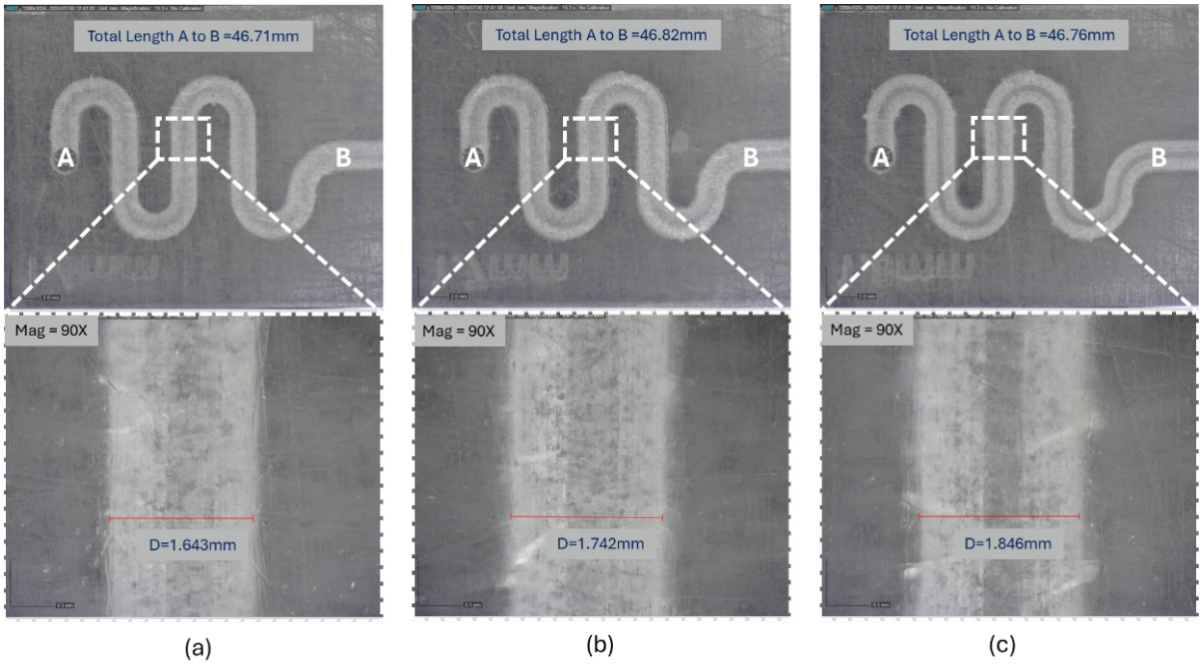

Figure 8. 3D-printed fluidic channels with three different channel diameters: (a) 1.6 mm channel diameter (b) 1.7 mm channel diameter c) 1.8 mm channel diameter.

Table 3 shows the summary of the flow time of the red-colored fluid from A to B, as well as the expected and measured values for all three channels. The measured dimension of the fabricated fluidic channels in terms of channel diameter and length is also shown in Table 3. It can be observed that the actual channel lengths of 46.71 mm (diameter 1.6 mm), 46.82 mm (diameter 1.7 mm), and 46.76 mm (diameter 1.8 mm) were slightly larger than the expected value (46.56 mm) due to fabrication tolerances. As a result, the measured flow times for all channel diameters were slightly different from the expected 35 minutes. The fluidic channel with a 1.6 mm diameter shows the closest flow time of 34.33 min to the expected value (35 minutes) with a percentage deviation of 1.91% compared to the other channels. Subsequently, the overall flow rate of the fluidic channel with a 1.6 mm channel diameter shows the most optimum value from the others with a percentage deviation of 7.87%.

Table 3. Summary of the flow time of the red-colored fluid from A to B and the measured dimensions for all channel diameters

Channel diameter [mm]		**Channel Length from A to B [mm]**		**Flow time A to B [min]**			**Overall Flow Rate [mm^3/min]**		
Expected	Measured	Expected	Measured	Expected	Measured	Percentage deviation [%]	Expected	Measured	Percentage deviation [%]
1.60	1.64	46.56	46.71	35.00	34.33	1.91	2.67	2.88	7.87
1.70	1.74	46.56	46.82	35.00	30.14	13.89	3.02	3.68	21.85
1.80	1.85	46.56	46.76	35.00	30.09	14.03	3.39	4.17	23.00

4.2. Results of Measurements for Heating Elements

Selecting the appropriate heating elements is crucial to attain the optimal temperature for the LAMP process quickly. The experiment compared three distinct heating elements: PTC heater 230, PTC heater 140, and heater cartridge. The heater's temperature was measured using

https://doi.org/10.31436/iiumej.v26i1.3407

a thermocouple and microcontroller. The temperature profiles for each heating element's heating process over five minutes are shown in Figure 9(a). The durations for the heating elements to achieve 65°C were as follows: PTC heater 230 (54.78 seconds), Heater Cartridge (78.41 seconds), and PTC heater 140 (149.07 seconds). PTC 230 heating element was chosen for its rapid heating performance (reaching 65°C in 54.78 seconds). As shown in Figure 9(a), the R2 values obtained are close to 1, which indicates the accuracy of the time value obtained at 65°C for all heaters.

The PTC 230 was further tested under an infrared thermal imaging camera to observe the uniformity of heat distribution of the heating element when it reaches 65°C, as shown in Figure 9(b) and Figure 9(c). The images clearly demonstrate a consistent and minimal temperature gradient across the heating element surface when it reaches 65°C. The highest temperature is observed at the center, gradually decreasing towards the edges. This indicates a uniform heat distribution pattern. Given that the temperature variation between the center and edges is only 1°C, or ±0.5°C from the center temperature, it can be concluded that the tolerance for the expected temperature value of 65°C for the LAMP process is within an acceptable range. The calculated tolerance of ±0.5°C accurately reflects this minimal temperature variation and ensures that the heating element operates within the specified temperature limits for the LAMP process. These experiments show that the fluidic channel system can be placed on top of the heating element, allowing the simultaneous flow and heating of the fluidic sample for 35 minutes at 65°C. It is also suitable for portable LAMP devices.

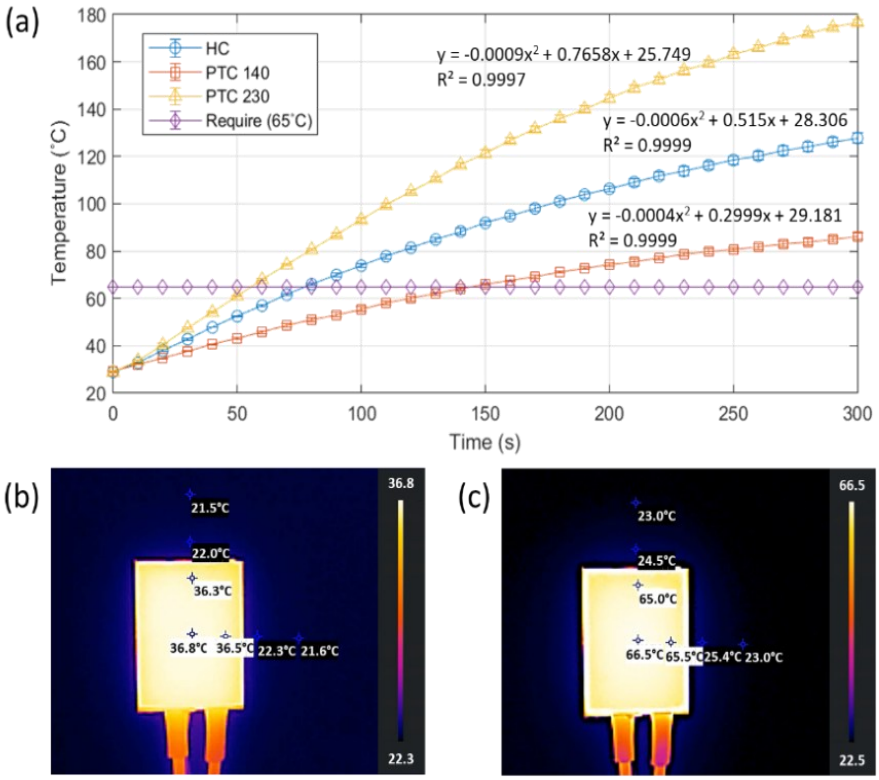

Figure 9(a) Temperature versus heating time for HC, PTC 140, and PTC 230 heating elements. (b) Thermal imaging of PTC 230 after 10 seconds of heating. (c) Thermal imaging of PTC 230 after 55 seconds of heating (reaching 65°C LAMP temperature).

The developed portable LAMP device, which consists of the PTC 230 heater and the fluidic channel, was used for DNA amplification of COVID-19 samples (74 positive, 74

negative) for COVID-19 detection using gold nanoparticle SPCE (AuNP-SPCE) electrochemical measurement, as reported in [4].

Table 4. Comparison of existing LAMP microfluidic devices with our work

Technology	Material used for microfluidic device	Fabrication Method	Sealing method	Remarks	Ref
Self-driven microfluidic chip	PDMS with hydrophilic UV-cured glue	Photolithography, spin-coating, oxygen plasma treatment, and bonding	Closed the channel with an air-control channel via a vacuum system	Complex fabrication. LAMP process of 56°C for 30 minutes for fluorescent detection of vancomycin-resistant enterococcus strain (VRE).	[6]
SlipChip / sp-SlipChip	Two layers of glass plate	Photolithography and thin-film deposition	Lubricating oils were placed between two plates	Complex fabrication. LAMP process of 65°C for 60 minutes for fluorescent detection of human papillomavirus (HPV-16 and HPV-18).	[7]
Smartphone-based multiplex test	Silicon wafer with SiO2 film	Photolithography, etching (Bosch process), thermal oxidation and dicing	Sealed with a double side adhesive layer and covered with glass on top	Complex fabrication. LAMP process of 65°C for 30 minutes to detect live virus from nasal swab extract.	[8]
Mask Stereolithography Fluidic	PMMA-like Resin	3D printing (MSLA)	Magnet Lid and PDMS sample well	Simpler method of 3D printed fabrication. LAMP process of 65°C for 35 minutes of COVID-19 detection using electrochemical measurement.	This work

Table 4 provides a detailed comparison of various LAMP microfluidic devices and highlights the advantages of our work. Existing technologies, such as self-driven microfluidic chips, SlipChip, and smartphone-based multiplex tests, demonstrate complex fabrication methods that rely on photolithography, spin-coating, thin-film deposition, and chemical etching processes. These methods involve multiple steps, such as thermal oxidation, vacuum systems, and lubricating oils for sealing. While these approaches have enabled precise control over the LAMP process, such as maintaining temperatures between 56°C and 65°C for 30–60 minutes, they are often labor-intensive, require specialized equipment, and lack the accessibility needed for widespread deployment, especially in low-resource settings. Additionally, these devices primarily focus on fluorescence detection, which can be cost-prohibitive and requires trained personnel for analysis.

In contrast, our work introduces a 3D-printed LAMP microfluidic device fabricated using a Mask Stereolithography Apparatus (MSLA). Utilizing PMMA-like resin and a simple magnet-lid sealing mechanism with a PDMS sample well significantly simplifies the fabrication process. Unlike conventional methods, our device eliminates the need for

photolithography and bonding techniques, reducing fabrication complexity and costs. The magnet lid and PDMS sample will also provide an innovative sealing solution that ensures leak-proof operation and facilitates fluidic sample flow directly to the sensor electrodes without manual intervention. This design simplifies the user experience and ensures compatibility with the LAMP process, which is maintained at 65°C for 35 minutes for COVID-19 detection using electrochemical measurement.

Furthermore, the performance of our device demonstrates that simplification in fabrication and operation does not compromise the sensor's accuracy or efficiency. Compared to existing devices, our system offers a seamless integration of the LAMP process with electrochemical detection, eliminating manual pipetting between steps. This reduces the risk of contamination while enhancing the device's usability in point-of-care settings. Our 3D-printed LAMP device thus represents a significant step forward in developing accessible and portable diagnostic tools, bridging the gap between complex laboratory-grade systems and practical, low-cost alternatives suitable for real-world applications.

5. CONCLUSION

This study successfully developed a 3D-printed serpentine fluidic channel integrated with a heating element. Leveraging the precision of MSLA 3D printing, a PMMA-like resin was used to fabricate a channel with an optimized diameter of 1.6 mm due to its minimal deviations in channel length (0.32%), flow time (1.91%) and overall flow rate (7.87%) as compared to 1.7 mm and 1.8 mm channels. Fluidic performance testing demonstrated fluidic flow at 2.88 µL/min flow rate without any leakage. Integrating a PTC 230 heating element has enabled rapid temperature control, reaching 65°C in 54.78 seconds. These results demonstrate the feasibility of producing a compact and efficient fluidic device suitable for portable applications. Future research will focus on enhancing the precision and reliability of the fluidic channel device and exploring different heating element options for improved performance. Implementing a flow rate sensor and pressure-driven system could contribute to a more consistent fluid flow within the device. Additionally, exploring fabrication techniques with different materials may enable the production of channels with more precise diameters, thereby improving the overall device performance.

ACKNOWLEDGEMENT

This research project was funded by the Ministry of Science, Technology, and Innovation (MOSTI) under the Combating COVID-19 Fund (project number: CV 02211032) grant and Ministry of Higher Education (MOHE) Fundamental Research Grant Scheme FRGS21-239-0848 (FRGS/1/2021/TK0/UIAM/02/9).

REFERENCES

[1] NAKAYAMA T, SOGA K (2023) Simple and quick detection of extended-spectrum β-lactamase and carbapenemase-encoding genes using isothermal nucleic acid amplification techniques. Journal of Microorganism Control 28:145–152. https://doi.org/10.4265/jmc.28.4_145

[2] Rahman MT, Uddin MS, Sultana R, Moue A, Setu M (2013) Polymerase Chain Reaction (PCR): A Short Review. Anwer Khan Modern Medical College Journal 4:30–36. https://doi.org/10.3329/AKMMCJ.V4I1.13682

[3] Kumar A, Venkatesan G (2018) Isothermal Nucleic Acid Amplification System: An Update on Methods and Applications Evaluation of immunogenicity and diagnostic potential of

recombinant proteins of Buffalopox virus View project Genetic characterization of virulence genes of orf virus isolates from sheep and goats View project. J Genet Genom 2:

[4] Zulhairee M, Zain RM, Nor ACM, Jafar NF, Noh MFM, Noorden MSA, Nordin AN, Rahim RA, Gunawan TS, Chin LY, Mohd Y, Azman NA, Zain ZM (2023) Clinical Performance of Reverse Transcription Loop-mediated Isothermal Amplification COVID-19 Assay on Gold-nanoparticle-modified Screen-printed Carbon Electrode Using Differential Pulse Voltammetry. Sensors and Materials 35:4731–4750. https://doi.org/10.18494/SAM4430

[5] Lin PH, Li BR (2021) Passively driven microfluidic device with simple operation in the development of nanolitre droplet assay in nucleic acid detection. Scientific Reports 2021 11:1 11:1–11. https://doi.org/10.1038/s41598-021-00470-9

[6] Ma YD, Chang WH, Luo K, Wang CH, Liu SY, Yen WH, Lee G Bin (2018) Digital quantification of DNA via isothermal amplification on a self-driven microfluidic chip featuring hydrophilic film-coated polydimethylsiloxane. Biosens Bioelectron 99:547–554. https://doi.org/10.1016/J.BIOS.2017.08.026

[7] Yu Z, Lyu W, Yu M, Wang Q, Qu H, Ismagilov RF, Han X, Lai D, Shen F (2020) Self-partitioning SlipChip for slip-induced droplet formation and human papillomavirus viral load quantification with digital LAMP. Biosens Bioelectron 155:112107. https://doi.org/10.1016/J.BIOS.2020.112107

[8] Sun F, Ganguli A, Nguyen J, Brisbin R, Shanmugam K, Hirschberg DL, Wheeler MB, Bashir R, Nash DM, Cunningham BT (2020) Smartphone-based multiplex 30-minute nucleic acid test of live virus from nasal swab extract. Lab Chip 20:1621–1627. https://doi.org/10.1039/D0LC00304B

[9] Nielsen A V., Beauchamp MJ, Nordin GP, Woolley AT (2020) 3D Printed Microfluidics. Annu Rev Anal Chem (Palo Alto Calif) 13:45. https://doi.org/10.1146/ANNUREV-ANCHEM-091619-102649

[10] Gale BK, Jafek AR, Lambert CJ, Goenner BL, Moghimifam H, Nze UC, Kamarapu SK (2018) A review of current methods in microfluidic device fabrication and future commercialization prospects. Inventions 3:. https://doi.org/10.3390/inventions3030060

[11] Luo F, Lei L, Cheng Z, Wan L, Zhao C, Niu K, Li C, Chen Q, Liu L, Wang N (2022) Magnet-actuated microfluidic reactors with controllable Fe-based amorphous microspheres for tetracycline degradation. J Flow Chem 12:297–305. https://doi.org/10.1007/S41981-022-00227-Z/METRICS

[12] Price AJN, Capel AJ, Lee RJ, Pradel P, Christie SDR (2021) An open source toolkit for 3D printed fluidics. J Flow Chem 11:37–51. https://doi.org/10.1007/S41981-020-00117-2/FigureURES/10

[13] Enders A, Siller IG, Urmann K, Hoffmann MR, Bahnemann J (2019) 3D Printed Microfluidic Mixers—A Comparative Study on Mixing Unit Performances. Small 15:1–9. https://doi.org/10.1002/smll.201804326

[14] Chen C, Mehl BT, Munshi AS, Townsend AD, Spence DM, Martin RS (2016) 3D-printed microfluidic devices: fabrication, advantages and limitations - a mini review. Analytical Methods 8:6005–6012

[15] Donia A, Furqan Shahid M, Hassan S ul, Shahid R, Ahmad A, Javed A, Nawaz M, Yaqub T, Bokhari H (2022) Integration of RT-LAMP and Microfluidic Technology for Detection of SARS-CoV-2 in Wastewater as an Advanced Point-of-Care Platform. Food Environ Virol 14:364–373. https://doi.org/10.1007/S12560-022-09522-3/FigureURES/1

[16] Lim J, Stavins R, Kindratenko V, Baek J, Wang L, White K, Kumar J, Valera E, King WP, Bashir R (2022) Microfluidic point-of-care device for detection of early strains and B.1.1.7 variant of SARS-CoV-2 virus. Lab Chip 22:1297–1309. https://doi.org/10.1039/D2LC00021K

[17] Lu S, Duplat D, Benitez-Bolivar P, León C, Villota SD, Veloz-Villavicencio E, Arévalo V, Jaenes K, Guo Y, Cicek S, Robinson L, Peidis P, Pearson JD, Woodgett J, Mazzulli T, Ponce P, Restrepo S, González JM, Bernal A, Guevara-Suarez M, Pardee K, Cevallos VE, González C, Bremner R (2022) Multicenter international assessment of a SARS-CoV-2 RT-LAMP test for point of care clinical application. PLoS One 17:. https://doi.org/10.1371/JOURNAL.PONE.0268340

[18] Ramírez-Chavarría RG, Castillo-Villanueva E, Alvarez-Serna BE, Carrillo-Reyes J, Ramírez-Zamora RM, Buitrón G, Alvarez-Icaza L (2022) Loop-mediated isothermal amplification-based electrochemical sensor for detecting SARS-CoV-2 in wastewater samples. J Environ Chem Eng 10:. https://doi.org/10.1016/j.jece.2022.107488

[19] Rocha RG, Silva ICOF, Arantes LC, Stefano JS, Lima CD, Melo LMA, Munoz RAA, dos Santos WTP, Richter EM (2021) Simple and rapid electrochemical detection of 1-benzylpiperazine on carbon screen-printed electrode. Microchemical Journal 167:1–7. https://doi.org/10.1016/j.microc.2021.106282

[20] Boselli E, Wu Z, Haynes EN, Papautsky I (2024) Screen-Printed Sensors Modified with Nafion and Mesoporous Carbon for Electrochemical Detection of Lead in Blood. J Electrochem Soc 171:027513. https://doi.org/10.1149/1945-7111/ad2397